Electronic Supplementary Information

Fabrication of Antifouling Polymer-Inorganic Hybrid Membranes through Synergy of Biomimetic Mineralization and Nonsolvent Induced Phase Separation

Xueting Zhao[a,b], Yanlei Su[a,b], Jialin Cao[a,b], Yafei Li[a,b], Runnan Zhang[a,b], Yanan Liu[a,b], Zhongyi Jiang[a,b,*]

[a] *Key Laboratory for Green Chemical Technology of Ministry of Education, School of Chemical Engineering and Technology, Tianjin University, Tianjin 300072, China*

[b] *Collaborative Innovation Center of Chemical Science and Engineering (Tianjin), Tianjin 300072, China*

[*] Corresponding author. School of Chemical Engineering and Technology, Tianjin University, No. 92, Weijin Road, Nankai District, Tianjin 300072, China
Tel: 86-22-27406646. Fax: 86-22-27406646.
E-mail address: zhyjiang@tju.edu.cn (Z.Y. Jiang)

S1. Synthesis of PVDF-g-PTA Copolymer, PVDF-g-xPHFBM-PTA Copolymer, and Fluorinated Triethoxysilane Precursor

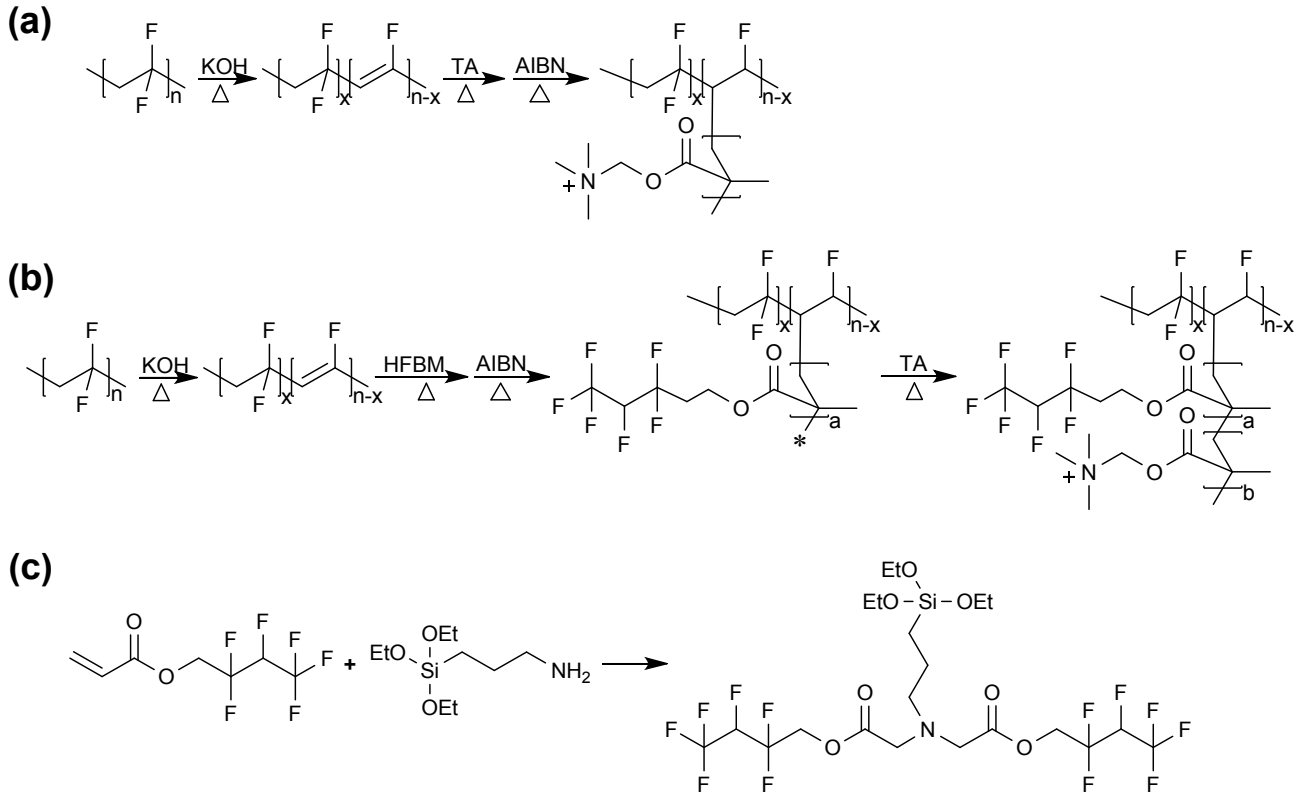

Fig. S1 Synthesis scheme for (a) PVDF-g-PTA copolymer, (b) PVDF-g-xPHFBM-PTA copolymer, and (c) fluorinated triethoxysilane precursor FTS.

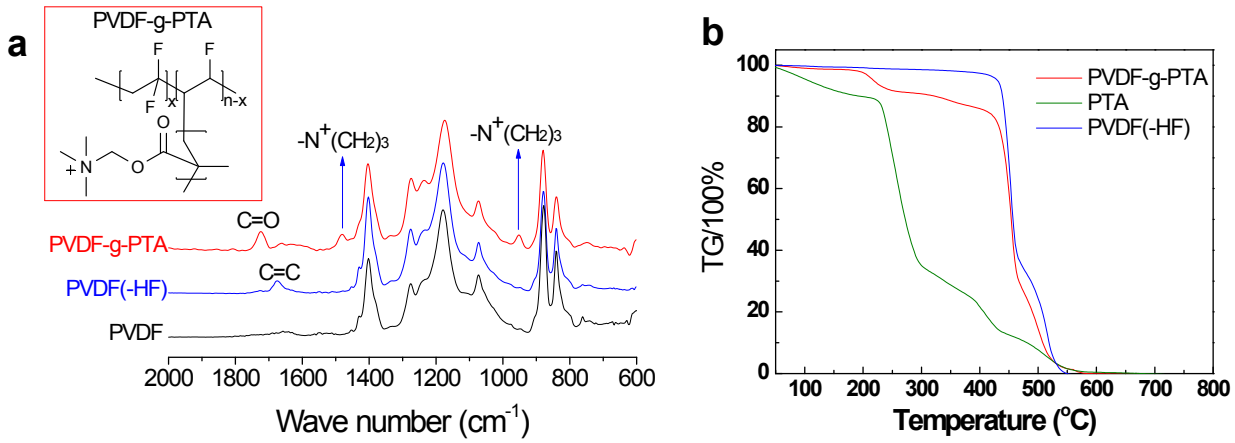

Fig. S2 (a) ATR-FTIR spectra of PVDF, PVDF(-HF) treated with KOH, and PVDF-g-PTA copolymer. Inset: chemical structure of PVDF-g-PTA copolymer, (b) TG curves of PVDF-g-PTA copolymer, PTA and PVDF(-HF).

The chemical structure and ATR-FTIR spectrum of PVDF-g-PTA copolymer were shown in Fig. S2(a).

The peak of C=C double bond at 1675 cm^{-1} in the spectrum of PVDF(-HF) became quite weak when copolymerized with monomer TA. Peaks at 1479 cm^{-1} and 952 cm^{-1} were related to the quaternary ammonium groups in PTA chain. The peak at 1723 cm^{-1} appeared in the spectra of PVDF-g-PTA was attributed to the C=O bonds from PTA chain. TGA measurements were performed to determine grafting degree of PTA Fig. S2(b). The decomposition of PTA appeared at the beginning, and 60.3 wt% weight loss of PTA was obtained after the second stage of decomposition with the temperature of 287.3 °C. The decomposition of PVDF(-HF) appeared at 440 °C. The weight percentage of grafted PTA segments in PVDF-g-PTA copolymer was calculated about 14.6 wt%.

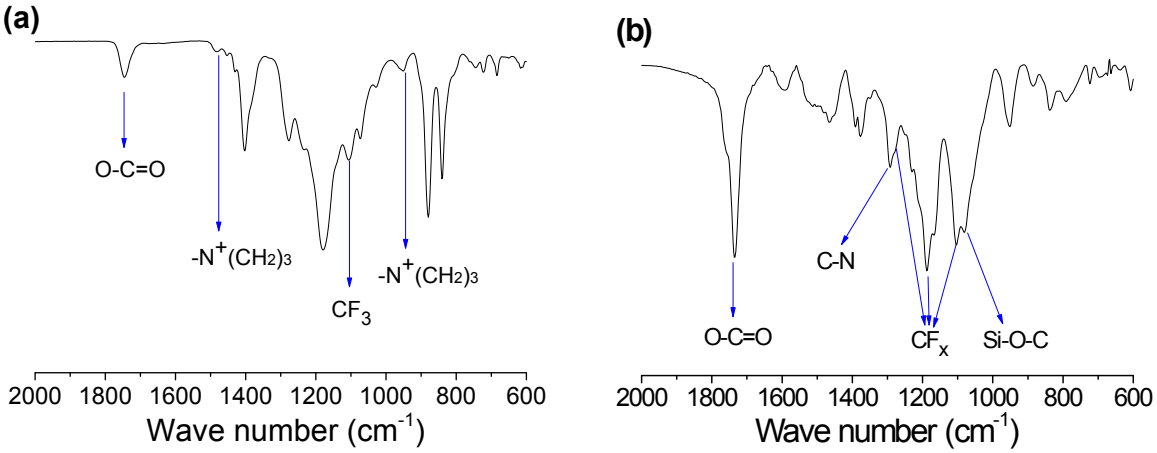

Fig. S3 ATR-FTIR spectra for (a) PVDF-g-PHFBM-PTA copolymer, and (b) fluorinated triethoxysilane precursor FTS.

For PVDF-g-PHFBM-PTA copolymer, the absorption band at 1745 cm^{-1} and 1100 cm^{-1} was assigned to the C=O stretching and CF_3 symmetric stretching from PHFBM segments, respectively; The peak at 1486 cm^{-1} and 945 cm^{-1} was assigned to the bending and stretching vibration of methyl groups of ammonium from PTA segments. For fluorinated triethoxysilane precursor FTS, the peak at 1745 cm^{-1} was contributed to the C=O stretching of PHFBA segments; the peaks at 1278 cm^{-1}, 1185 cm^{-1}, and 1101 cm^{-1} were characteristic of CF_x symmetric stretching in PHFBA segments; The peak at 1079 cm^{-1} was assigned to the Si-O-C stretching from APTS; The absorption peaks at 1291 cm^{-1} belonged to C–N

stretching mode from APTS; No deformation vibration of N-H was observed at 1650 cm^{-1} indicated that primary amines reacted with two equivalents of acceptor to form tertiary amines.

S2 *In Situ* Biomimetic Mineralization during Membrane Preparation

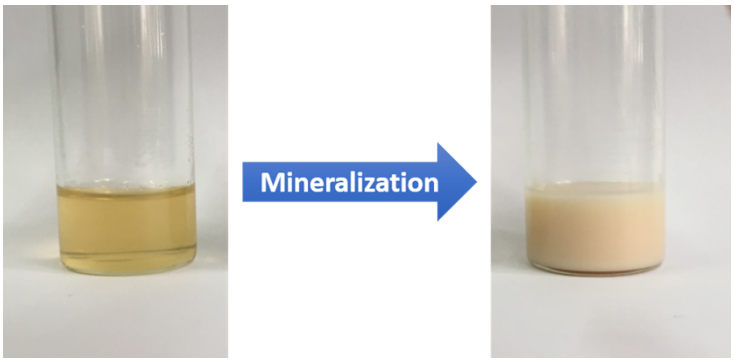

Fig. S4 Digital photo of PVDF-g-PTA/NMP membrane casting solution and PVDF-g-PTA/NMP/TALH(H_2O) membrane casting solution after 12 h of mineralization. The equal amount of water was added in PVDF-g-PTA/NMP membrane casting solution to eliminate the influence of water.

S3 Characterizations of the PVDF-g-PTA/TiO_2 Hybrid Membranes

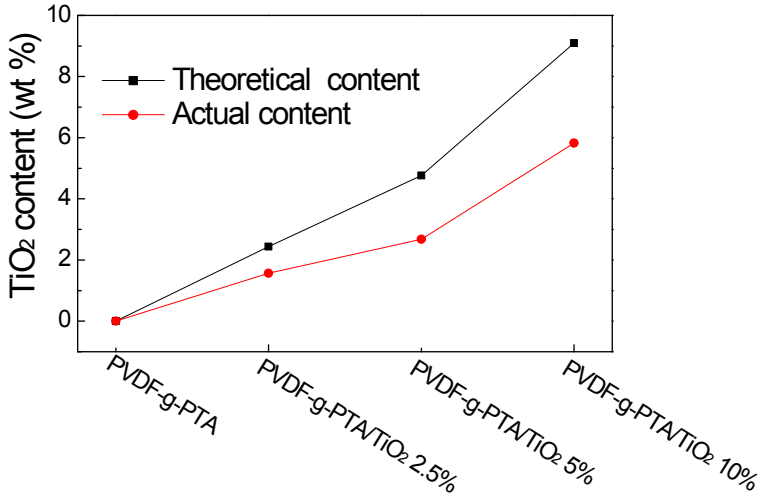

Fig. S5 The actual contents (from TGA), and theoretical contents (from casting solution composition) of TiO_2 NPs in PVDF-g-PTA/TiO_2 hybrid membranes.

Table S1 Elements analysis results of PVDF-g-PTA/TiO_2 hybrid membranes determined by XPS and the bulk elemental compositions of Ti in membranes determined by TGA.

Membranes	C (wt %)	N (wt %)	O (wt %)	F (wt %)	Ti (wt %)	Ti^{TGA} (wt %)	Ti/Ti^{TGA}
PVDF-g-PTA/TiO_2 2.5%	42.96	1.82	9.97	42.51	2.74	0.94	2.91
PVDF-g-PTA/TiO_2 5%	46.75	2.32	10.65	36.00	4.28	1.61	2.66
PVDF-g-PTA/TiO_2 10%	52.82	6.21	19.58	14.16	7.22	3.49	2.17

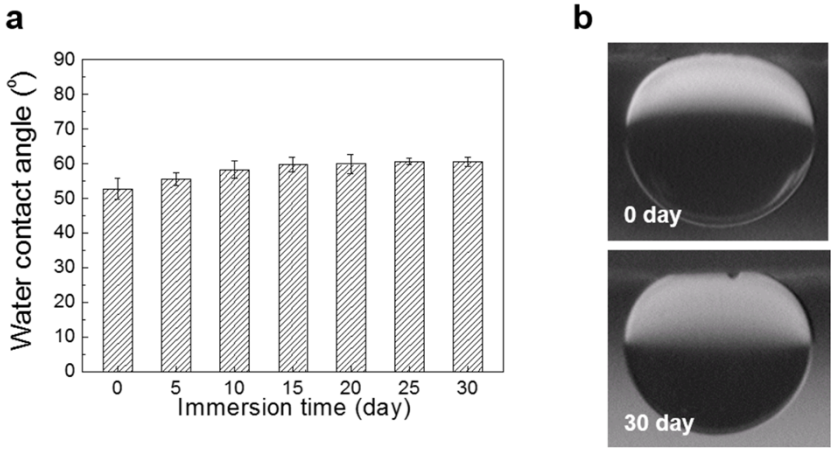

Fig. S6 The hydrophilicity (a) and superoleophobicity (b) of PVDF-g-PTA/TiO_2 10% hybrid membrane surface after shaken (100 rpm) in the water for 30 days.

S4 Characterizations of the PVDF-g-PHFBM-PTA/TiO_2 and PVDF-g-PTA/TiO_2-FTS Hybrid Membranes

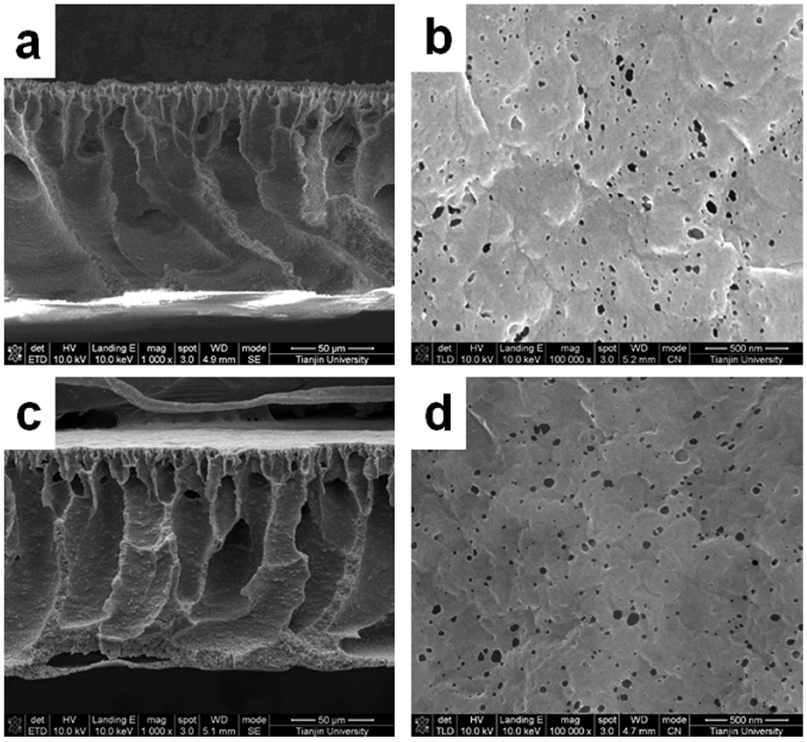

Fig. S7 Cross-section and surface morphologies of (a, b) PVDF-g-xPHFBM-PTA/TiO_2 hybrid membrane (x=1) and (c, d) PVDF-g-PTA/TiO_2-xFTS hybrid membrane (x=1).

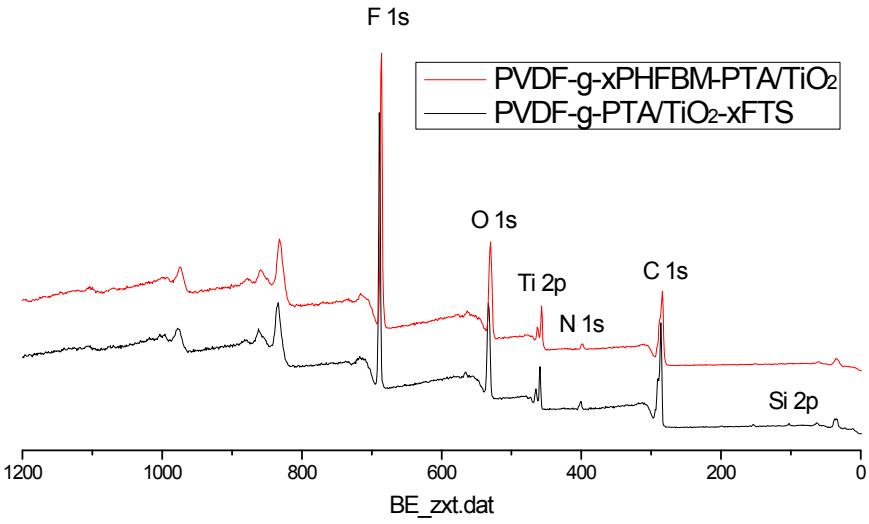

Fig. S8 Wide scan XPS spectrum of PVDF-g-xPHFBM-PTA/TiO_2 and PVDF-g-PTA/TiO_2-xFTS hybrid membrane (x=1).

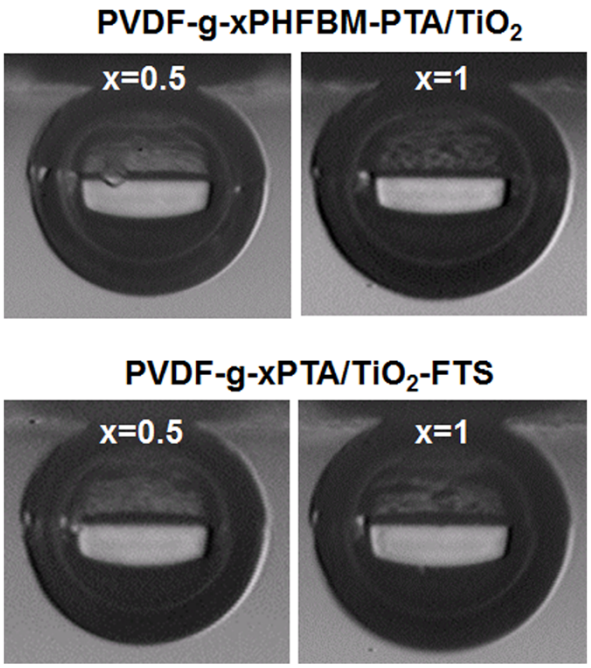

Fig. S9 Underwater captive air contact angles of PVDF-g-xPHFBM-PTA/TiO_2 and PVDF-g-PTA/TiO_2-xFTS hybrid membranes

The surface TiO_2 and -CF_3 contents were calculated as following:

Surface TiO_2 content=Ti %×3 (S1);

Surface -CF_3 content=φ×C %×4 (S2);

Ti % was the atom percentage of Ti element on membrane surfaces determined by XPS. The factor 3 accounted for the 3 atoms in TiO_2. C % was the atom percentage of C element on membrane surfaces determined by XPS. The factor 4 accounted for the 4 atoms in –CF_3. φ was the area ratio of the peak for –$\underline{C}F_3$ in C 1s XPS spectra.